

# A NEW ALGORITHM FOR DENSE TWO-FRAME STEREO CORRESPONDENCE

Ignazio Gallo, Elisabetta Binaghi

*Universita' degli Studi dell'Insubria, Varese, Italy*  
*elisabetta.binaghi@uninsubria.it, gallo@uninsubria.it*

**Abstract:** This work aims at defining a new method for matching correspondences in stereoscopic image analysis. The salient aspects of the method are -an explicit representation of occlusions driving the overall matching process and the use of neural adaptive technique in disparity computation. In particular, based on the taxonomy proposed by Scharstein and Szelinsky, the dense stereo matching process has been divided into three tasks: *matching cost computation*, *aggregation of local evidence* and *computation of disparity values*. Within the second phase a new strategy has been introduced in an attempt to improve reliability in computing disparity. An experiment was conducted to evaluate the solutions proposed. The experiment is based on an analysis of test images including data with a ground truth disparity map

**Keywords:** stereo, occlusion, disparity space, neural networks.

## 1. INTRODUCTION

The reconstruction of three-dimensional shape from two or more images is a well known and intensively investigated research problem within the Computer Vision community (Barnard and Fischler 1982; ; Dhond and Aggarwal 1989).

Major efforts have been devoted to the stereo matching sub-task aimed at computing correspondences in two (or more) images for obtaining dense depth maps. A substantial amount of work has been done on stereo matching giving rise to a variety of novel approaches (Scharstein and Szelisky, 2002) attempting to improve upon existing early methods and satisfy the high accuracy demand in diversified application domains such as object recognition, robotics and virtual reality (McMillan and Bishop 1995).

Despite important achievements, the accuracy of most innovative stereo techniques may not be adequate especially in those situations where even isolated errors in the depth map create visible undesirable artefacts. The problem originates from the fact that most stereo algorithms ignore occlusions analysis or address it in a post processing stage within a more general smoothing task (Bobik and Intille 1999).

Occlusions are widespread in stereo imagery and even when images with small disparity jumps are processed, they drastically affect the accuracy of the overall reconstruction process being the major source of errors.

Recent works on stereo matching stem from the idea of mimicking the human visual system which uses occlusions to reason about the spatial relationships between objects during binocular stereopsis. Explicit representation of occlusions and direct processing within occlusion edges characterizes these approaches (Bobik and Intille 1999).

This paper proposes a novel algorithm for solving stereo correspondence based on an explicit representation of occlusions driving the overall matching process. In particular, based on the taxonomy proposed by Scharstein and Szelinsky, the dense stereo matching process has been divided into three tasks: *matching cost computation*, *aggregation of local evidence* and *computation of disparity values* (Scharstein and Szelisky, 2002). Within the second phase a new strategy has been introduced in an attempt to improve reliability in computing disparity. An experiment was conducted to evaluate the solution proposed. The experiment is based on an analysis of test images including data with a ground truth disparity map and make use of the quality metrics proposed by Scharstein and Szelinsky (Scharstein and Szelisky, 2002).

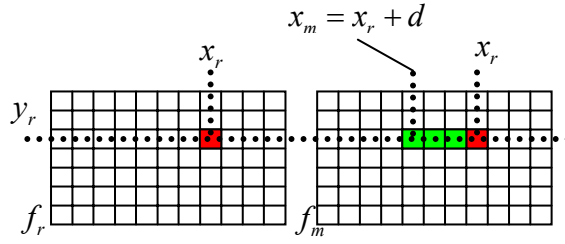


Figure 1 - Correspondence between a pixel  $(x_r, y_r)$  in reference image  $f_r$  and a pixel  $(x_m, y_r)$  in matching image  $f_m$ . The difference  $d = (x_m - x_r)$  is the disparity value.

## 2. REPRESENTATION

This section describes a data structure called *Disparity Space Image*, or *DSI*, already introduced in previous works (Okutomi and Kanade 1994; Bobik and Intille 1999). The DSI is an explicit representation of matching space and plays an essential role in the development of the overall matching algorithm which makes use of occlusion constraints.

The correspondence between pixel  $(x_r, y_r)$  in a Reference Image  $f_r$  and a pixel  $(x_m, y_m)$  in a Matching Image  $f_m$  is defined as

$$f_r(x_r, y_r) = f_m[x_r + s \cdot d(x_r, y_r), y_r] + \eta(x_r, y_r) \quad (1)$$

where  $s = \pm 1$  is a sign chosen so that disparities are always positive;  $d(x_r, y_r)$  is the disparity function and  $\eta(x_r, y_r)$  is the Gaussian white noise.

From equation (1) we obtain

$$x_m = x_r + s \cdot d(x_r, y_r) \quad (2)$$

and from equation (2):

$$d(x_r, y_r) = s \cdot (x_m - x_r) \quad (3)$$

Introducing the *epipolar constraint*, we also have:

$$y_r = y_m \quad (4)$$

supposing the pixels move from right to left.

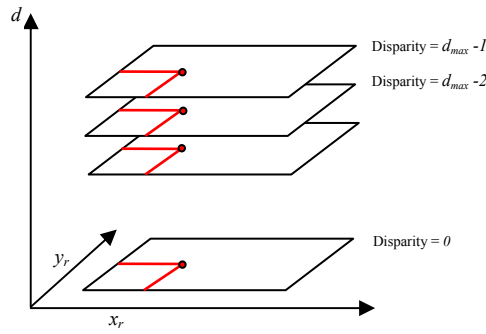


Figure 2 - Graphic Representation of Disparity Space Image (DSI)

Once the disparity space has been specified, the concept of DSI can be introduced and defined as any image or function over the disparity space  $(x_r, y_r, d)$ . Values of DSI usually represent the *cost of a* particular match implied by the particular  $d(x, y)$  considered.

Figure 2 shows a graphic representation of DSI: each slice indicates a level of disparity varying from 0 to a value  $d_{\max}$  representing the maximum disparity for the pair of images considered.

### 3. GROWING TEMPLATE ALGORITHM

According to the taxonomy proposed by Scharstein and Szelinsky, the dense stereo matching process can be divided into four tasks (Scharstein and Szelisky, 2002):

- 1) *Matching Cost Computation*
- 2) *Aggregation Cost*
- 3) *Disparity Computation and Optimization*
- 4) *Disparity Refinement*

Many dense stereo matching methods have presented several different solutions to one or more of these tasks. The most common *matching costs* include *squared intensity differences (SD)* and *absolute intensity difference (AD)* (Cox et al., 1996; Scharstein and Szelisky, 2002).

The actual sequence of steps in the overall matching procedure depends on the matching algorithm and in particular, on its local or global nature.

Our approach, which follows a local strategy, extends the conventional Aggregation Cost phase including two novel sub-tasks:

- 2.1) *Growing Raw Cost*
- 2.2) *Growing Aggregation Cost*

#### 3.1 Matching Cost Computation

Assuming the use of SD as matching function, by equation (3) the matching cost computed for a pixel  $(x_r, y_r)$  is defined as:

$$DSI(x_r, y_r, d) = [f_r(x_r, y_r) - f_m(x_m, y_r)]^2 \quad (5)$$

where  $d$  is the disparity associated with the pixel  $(x_r, y_r)$  and  $0 \leq d \leq d_{\max}$ .

### 3.2 Aggregation Cost

Local and window-based methods aggregate the matching cost by summing or averaging over a support region in the DSI. The support region we use is a two-dimensional squared window of a fixed dimension.

In particular, this second step is performed by summing the calculated matching costs over a squared window with constant disparity  $\bar{d}$ . The aggregation cost  $AC_{i,j}^d$  is defined as:

$$AC_{i,j}^{\bar{d}} = \sum_{m=a}^{a+W} \sum_{n=b}^{b+W} DSI(m, n, \bar{d}) \quad (6)$$

where  $a = \left(i - \frac{W}{2}\right)$  and  $b = \left(j - \frac{W}{2}\right)$ .

Considering all the aggregation values obtained varying the disparity in the range  $[0 \dots d_{\max}]$ , we obtain:

$$\overrightarrow{AC}_{m,n} = [AC_{m,n}^0, AC_{m,n}^1, \dots, AC_{m,n}^{d_{\max}}] \quad (7)$$

A classic Stereo Matching Algorithm, at this point, with a WTA technique for example, decides that the disparity is computed by selecting the minimal aggregated cost in  $\overrightarrow{AC}_{m,n}$ . The Growing Template Algorithm adds two new steps at the aggregation cost phase.

We now describe the two parts that characterize the Growing Template Aggregation Cost step.

### 3.3 Growing Raw Cost

Unlike conventional techniques that base further steps of matching algorithm on the minimal aggregated cost computed in  $\overrightarrow{AC}_{m,n}$ , our approach bases decisions on all the costs obtained. To this purpose, we introduce a new quantity  $\overrightarrow{RC}_{m,n}$  defined as

$$\overrightarrow{RC}_{m,n} = [RC_{m,n}^0, RC_{m,n}^1, \dots, RC_{m,n}^{d_{\max}}] \quad (8)$$

where each element indicates the position in the sorted list of the element  $AC_{i,j}^d$

For example, if we have the vector  $\overrightarrow{AC}_{m,n} = [12, 1, 16]$  the corresponding vector of raw cost is  $\overrightarrow{RC}_{m,n} = [2, 1, 3]$ .

At the end of this phase for every pixel of coordinates  $(m, n)$  in the reference image we have associated the  $\overrightarrow{RC}_{m,n}$  calculated.

### 3.4 Growing Aggregation cost

This sub-task calculates the number of confirmations in a given support window for a given cost  $l$ . Formally, from equation (8) we obtain the vector:

$$\overline{GA}_{m,n} = [GA_{m,n}^0, GA_{m,n}^1, \dots, GA_{m,n}^{d_{\max}}] \quad (9)$$

where

$$GA_{m,n}^d = \sum_{(m,n) \in W \times W} (RC_{m,n}^d \leq l) \quad (10)$$

The salient aspect of our strategy is that of integrating contextual confirmation within the matching cost aggregation phase. The aggregation can be performed based on different cost values varying the  $l$  parameter in equation 10.

Figure 3 compares DSI's slices for fixed  $y$  obtained by means of a matching algorithm including conventional aggregation cost computation (a) and our algorithm which includes the growing aggregation task (b). Both figures 3a and 3b highlight bands (dark lines and white lines respectively) indicating regions that match at a given disparity. They are more visible in figure 3a depicting disparity and occlusion situations without ambiguity.



Figure 3 – DSI's slices obtained from a conventional stereo matching algorithm (a), and obtained by the growing aggregation algorithm (b)

### 3.5 Disparity Computation

The next phase in the matching algorithm consists in the computation of the disparity map by selecting the  $\overline{GA}_{m,n}$  components which satisfy a given criterion. Adopting a Winner Take All strategy, the disparity associated with the minimum cost value is selected at each pixel.

The present work tested an adaptive strategy based on *neural networks* for disparity computation. A Multilayer Perceptron neural model was adopted to compute the disparity based on specific local information extracted from the DSI slice.

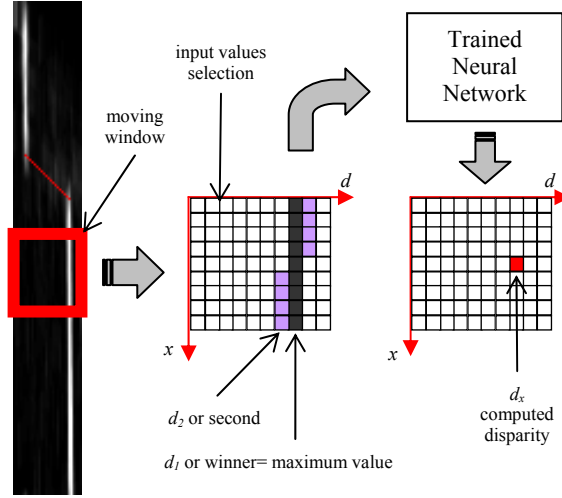


Figure 4 –Disparity computation procedure based on a trained neural network. The process extracts patterns from a window positioned over a DSI slice. For each  $x$  we select two values:  $d_1$  and  $d_2$ . The trained neural network calculates the disparity associated with the center of the moving window.

The network is trained receiving input data from the DSI slices. In particular, at each position of a moving window over the DSI slice, an input pattern is extracted and presented to the network. A training example is constituted by a pair of elements  $(a, b)$  where  $a$  is the input pattern collecting a set  $\{d_i\}$  and  $b$  corresponding disparity extracted from ground truth image for each  $x$  within the moving window. (Figure 4).

#### 4. EXPERIMENTS

The experiments illustrated in this section addressed the following questions:

- how did the performance depend upon their main parameters and upon the neural refinement stage?
- how did the Growing Template Algorithm compare with other matching approaches?

The overall experimental activity was supported by tools and test data available within the implementation framework proposed by Scharstein & Szelinski in their paper (Scharstein and Szelisky, 2002) and made available on the Web at [www.middlebury.edu/stereo](http://www.middlebury.edu/stereo). We included our stereo correspondence algorithm in this framework, and applied it to the test data available.

Four stereo image pairs with different types of content are used to evaluate the performances of the proposed algorithm (see Figure 6).

Among the quality measures available within the framework, we adopted the RMS (root mean squared) error (measured in disparity units) between the computed disparity map  $d_C(x, y)$  and the ground truth map  $d_T(x, y)$

$$R = \left( \frac{1}{N} \sum (|d_C(x, y) - d_T(x, y)|^2) \right)^{\frac{1}{2}} \quad (12)$$

These measures are intended computed over the whole image and five different kinds of regions in the whole image:

- textureless regions (TEXTRD): regions where the squared horizontal intensity gradient averaged over a square window of a given size (suggested value 3) is below a given threshold (suggested value 4.0)
- textured regions (TEXTRLS): regions complementary to the textureless regions
- occluded regions (OCCL): regions that are occluded in the matching image
- non occluded regions (NONOCCL): regions complementary to the occluded regions

- depth discontinuity regions (DISC): pixels whose neighboring disparity differs by more than a given threshold (suggested value 2.0), dilated by a window of a given width (suggested value 9)
- These regions are computed by pre-processing reference images and ground truth disparity maps yielding binary segmentation.

## 4.1 Sensitivity Analysis

We attempted to evaluate the effects of systematically varying some of the key parameters of our stereo algorithm to find an optimal setting for all situations. Experiments were developed using SD and AD matching costs and windows of size 7, 15, 21, 35 for Growing Aggregation Cost.

Results obtained demonstrate that performances are not strongly influenced by the type of matching costs used. A large window can help for occlusion regions. Inversely, small windows perform better on discontinuity regions.

Dimensions of 35X35 were selected allotting the task of optimizing the balance between high accuracy in occlusion and discontinuity regions to the neural adaptive stage.

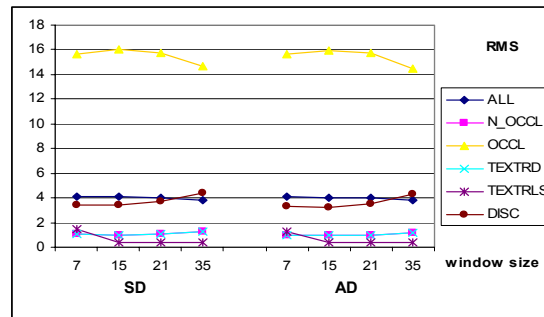


Figure 5 –Sensitivity Analysis of Growing Aggregation Algorithm

## 4.2 Performance Evaluation and Comparison Analysis

At first the evaluation procedure aimed to identify and evaluate the contribution of neural refinement within the global matching algorithm. To this purpose we compared the Growing Aggregation Algorithm including the neural stage with the same version including the WTA strategy for disparity computation. The evaluation was based on the monochromatic MAP pair of images.

As shown in Table 1, the algorithm with neural refinement (GA+N) strongly prevails in all regions considered.

We compared performances obtained by means of the Growing Aggregation Algorithm including neural refinement with those obtained by running four algorithms implemented within the cited framework available, selected among those with better performances.

Table 1 – Results obtained with MAP image. GA=Growing Aggregation, GA+N=Growing Aggregation+ Neural Network for disparity computation,

	ALL	NON OCCL	OCCL	TEXT RD	TEXT RLS	DISC
GA	3.85	1.31	14.88	1.32	0.40	4.69
GA+N	1.66	1.42	3.82	1.42	0.72	4.86

Table 2 – Results obtained with MAP image. SSD=Sum of Squared Difference, SO=Scanline Optimization, BD=Bayesian Diffusion

	ALL	NON OCCL	OCCL	TEXT RD	TEXT RLS	DISC
DP	3.15	2.98	5.21	2.99	1.75	5.86
SSD	3.92	1.66	14.65	1.67	0.44	6.07
SO	4.39	2.02	16.09	2.02	2.57	5.25
BD	4.66	0.93	18.74	0.94	0.43	2.95

Figure 7 shows final disparity maps obtained by processing the four stereo image pairs considered.

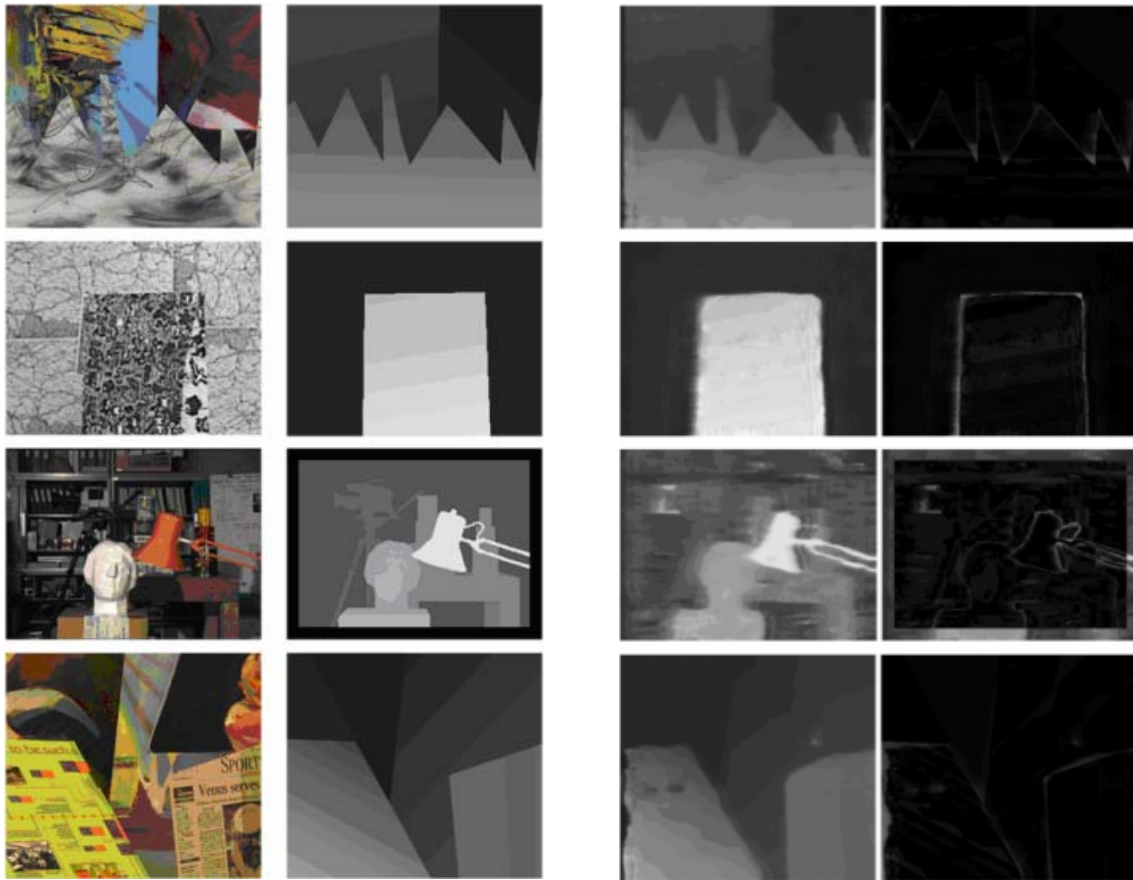


Figure 6 –Left image and ground truth disparity maps of test set

Figure 7 –Final disparity maps and difference images

## 5. CONCLUSIONS

Our objective in this study was to investigate the potentialities of a new method aimed at solving correspondence problem within a two-frame area matching approach and producing dense disparity maps.

The strategy was tested on standard data sets available on the Web. As seen in this experimental context the allied use of the growing aggregation strategy and neural adaptive techniques benefits the matching in general and in particular in occluded regions.

We consider this study preliminary to further investigation involving both methodological and experimental issues. For example, the present solutions must be reinforced implementing an operative strategy for training neural network.

Further experiments dealing with Scanning Electron Microscopy imagery are planned.

## 6. REFERENCES

- Barnard, S.T. and Fischler, M.A. Computational Stereo. *ACM Computing Surveys*, 14(4):553-572, 1982.
- Bishop, C.M. 1995. *Neural Networks for Pattern Recognition*, Oxford University Press, Oxford.
- Bobik, A. F and Intille, S. S.. 1999. Large occlusion stereo. *International Journal on Computer Vision*, 33, 181-200.
- Cox, J.I., S.L. Higonani, S.P. Rao, B.M. Maggs. 1996. A Maximum Likelihoods Stereo Algorithm. *Computer Vision and Image Understanding*, 63, 542-567.
- Dhond, U.R. and Aggarwal, J.K. 1989. Structure from Stereo – a review. *IEEE Trans. On Systems, Man, and Cybernetics*, 19, 1489-1510.
- McMillan, L. and Bishop, G. 1995. Plenoptic modelling: An image-based rendering system. *Computer Graphics (SIG-GRAPH'95)*, 39-46.
- Kanade, T. and Okutomi, M. 1994. A Stereo Matching Algorithm with an Adaptive Window: Theory and Experiment. *IEEE Trans. on PAMI*, 16(9), 920-932.
- Rumelhart, H., G.E. Hinton, and R.J. Williams. 1986. Learning Internal Representation by Error Propagation, in Rumelhart H., McClelland J.L. (eds.), *Parallel Distributed Processing*, 318-362. MIT Press, Cambridge, MA.
- Scharstein, D. and Szeliski R. 2002. A Taxonomy and Evaluation of Dense Two-Frame Stereo Correspondence Algorithms. *International Journal of Computer Vision*, 47, 7-42.